SIAM J. Appl. Math.
Vol. 80, No. 4, pp. 1607–1628

MINIMIZATION OF THE FIRST NONZERO EIGENVALUE PROBLEM FOR TWO-PHASE CONDUCTORS WITH NEUMANN BOUNDARY CONDITIONS*

DI KANG†, PATRICK CHOI‡, AND CHIU-YEN KAO§

Abstract. We consider the problem of minimizing the first nonzero eigenvalue of an elliptic operator with Neumann boundary conditions with respect to the distribution of two conducting materials with a prescribed area ratio in a given domain. In one dimension, we show monotone properties of the first nonzero eigenvalue with respect to various parameters and find the optimal distribution of two conducting materials on an interval under the assumption that the region that has lower conductivity is simply connected. On a rectangular domain in two dimensions, we show that the strip configuration of two conducting materials can be a local minimizer. For general domains, we propose a rearrangement algorithm to find the optimal distribution numerically. Many results on various domains are shown to demonstrate the efficiency and robustness of the algorithms. Topological changes of the optimal configurations are discussed on circles, ellipses, annuli, and L-shaped domains.

Key words. two-phase conductor, extremal eigenvalue problem, rearrangement algorithm, Neumann boundary conditions

AMS subject classifications. 49Q10, 35P15, 47J30, 49R50, 47A55

DOI. 10.1137/19M1251709

1. Introduction.

Optimization of eigenvalues in problems involving elliptic operators has been of interest to many researchers due to its usefulness in many applications including drum vibration [31, 16, 7, 42, 23, 22, 29], rod and plate vibration [4, 44, 3, 2, 20, 19, 8, 25], determination of favorable and unfavorable regions in population dynamics [35, 26, 24, 5, 10, 32], design of optical resonators [28, 36, 30, 34], bandgap optimization in photonic crystals [18, 17, 27, 45, 39, 43, 9, 38, 40], and two-phase conductors [15, 14, 13, 21, 12, 33]. In some applications, it is desirable to obtain optimal arrangement of different materials within a fixed domain so that a certain material property can be maximized or minimized. The property that needs to be optimized may be absorptivity, density, and electrical or thermal conductivity, just to name a few. These problems typically involve the careful choice of a cost function or an objective function subject to a certain set of constraints.

In this paper, we are interested in the problem of minimizing the first nonzero eigenvalue of an elliptic operator with respect to the distribution of two conducting materials with a prescribed area ratio in a domain. For the Dirichlet problem, the two-phase conductor problem is modeled as

$$\begin{cases} -\nabla \cdot (\sigma(x)\nabla u(x)) = \mu u(x) \quad \text{in } \Omega, \\ u = 0 \quad \text{on } \partial\Omega, \end{cases} \tag{1.1}$$

*Received by the editors March 29, 2019; accepted for publication (in revised form) April 14, 2020; published electronically July 1, 2020.
https://doi.org/10.1137/19M1251709
Funding: This work was supported by the NSF through grant DMS-1818948.
†Department of Mathematics and Statistics, McMaster University, Hamilton, ON L8S 4K1, Canada (kangd18@mcmaster.ca).
‡Institute of Mathematical Sciences, Claremont Graduate University, Claremont, CA 91711 (patchoi2@yahoo.com).
§Department of Mathematical Sciences, Claremont McKenna College, Claremont, CA 91711 (ckao@cmc.edu).

where $u(x)$ is the temperature function defined on a smooth domain $\Omega \subset \mathbb{R}^N$, σ is the conductivity function which satisfies

$$\sigma = \sigma_M \chi_D + \sigma_m \chi_{\Omega \backslash D}, \tag{1.2}$$

σ_M and σ_m are both constants, $\sigma_M > \sigma_m = 1$, and $D \subset \Omega$. The minimization of the ground state energy with respect to a two-phase conductor with a fixed area ratio is to find the first eigenvalue μ_1 that

$$\min_D \mu_1(D) \text{ such that } \frac{|D|}{|\Omega|} = \gamma, \tag{1.3}$$

where γ is a given constant.

In [1], the existence of the solution to problem (1.1)–(1.3) is established when Ω is a ball and the minimizer is shown to be a radially symmetric function. Later, a simpler proof based only on a rearrangement method was published in [13]. It is shown in [6] that if $\Omega \in \mathbb{R}^N$, is simply connected, and has a connected boundary, then problem (1.1)–(1.3) has a solution if and only if Ω is a ball. For other general domains, this problem remains open. In the class of relaxed designs, Cox and Lipton were able to show the existence of a solution [15]. In one dimension, if a two-phase conductor is considered on the interval $[0, 1]$, the minimizer has $D = [\frac{1-\gamma}{2}, \frac{1+\gamma}{2}]$ while the maximizer has $\Omega \backslash D = D^c = [\frac{1-\gamma}{2}, \frac{1+\gamma}{2}]$. When Ω is a ball, the existence of a radially symmetric optimal set has been proved in [1] by using rearrangement techniques. Even in this case an explicit solution to the problem is not known. It was conjectured in [13, 14] that the optimal high conductivity region D is a smaller ball centered in the domain, which is a ball. However, this conjecture is not true in general. It was proved in [12] that the optimal domain D cannot be a ball when σ_m and σ_M are close to each other and γ is sufficiently large. In this case, the optimal D consists of a ball centered in the domain and an outer ring attached to the boundary. In [41], the conjecture was proved to be false for the N-ball when $N \geq 2$. For domains such as a square, a cube, a crescent, and an ellipse with two holes, a rearrangement algorithm was proposed to find the optimal two-phase conductor with Dirichlet boundary conditions numerically [12, 11]. Alternatively, one can use the level set method to represent the interface between lower and higher conductivity regions and find the optimal interface by a gradient flow. This approach was used in [37] to find the optimal two-phase conductors for various boundary conditions.

In this paper, we study the optimal conductivity problem with Neumann boundary conditions. In one dimension, we explore the monotone properties of first nonzero eigenvalues with respect to the area ratio γ and the high conductivity value σ_M. We show that the optimal distribution of the material which has the minimal first nonzero eigenvalue is to have the high conductivity material placed evenly at two ends of the interval under the assumption that the region that has lower conductivity is simply connected. On a rectangular domain in two dimensions, we show that the set $D^c = \Omega \backslash D$ which has a strip configuration parallel to short edges is a local minimizer by an asymptotic approach. The Fourier series expressions of the eigenfunctions are obtained and the equations that determine eigenvalues are derived. A thorough comparison of eigenvalues to determine a local minimizer of a nonzero eigenvalue allows us to show that the one corresponding to the strip configuration is indeed a local minimizer under the assumption. For problems on general domains, we propose a rearrangement algorithm to find the optimal two-phase conductor. It generates a sequence of two-phase conductors whose corresponding eigenvalues form a monotone decreasing sequence which converges to the minimal value numerically. Many results on various domains are shown to demonstrate the efficiency and robustness of the algorithms. Topological changes of the optimal configurations are discussed on circles, ellipses, annuli, and L-shaped domains.

This paper is structured as follows: In section 2, we discuss the minimization of first nonzero Neumann-Laplacian eigenvalues in both one and two dimensions. In one dimension, several monotone properties of the eigenvalue are found for various parameters. We also show the approach to finding the minimizer analytically under certain assumption. On a rectangular domain in two dimensions, we perform an asymptotic analysis of the eigenvalue to show that a strip configuration of conductivity may be a local optimizer. In section 3, a rearrangement algorithm is proposed to find the optimal two-phase conductor, and numerical results on various domains are shown to demonstrate the efficiency and robustness of the algorithms. The paper is summarized with a brief conclusion in section 4.

2. Minimization of first nonzero Neumann-Laplacian eigenvalues. We will focus on the problem of finding the optimal conductivity distribution of materials consisting of two different conductivities with fixed proportions which has the smallest first nonzero Neumann-Laplacian eigenvalue. The governing equation is

$$\begin{cases} -\nabla \cdot (\sigma(\mathbf{x}) \nabla u(\mathbf{x})) = \nu u(\mathbf{x}), & \mathbf{x} \in \Omega, \\ \sigma \dfrac{\partial u(\mathbf{x})}{\partial n} = 0 \quad \text{for } \mathbf{x} \in \partial\,\Omega, \end{cases} \tag{2.1}$$

where σ is in the class of functions defined by

$$A_{\sigma_m,\sigma_M,\tau} := \left\{ \sigma(\mathbf{x}) = \sigma_M \chi_D + \sigma_m \chi_{\Omega \setminus D},\ D \subset \Omega; \int_\Omega \sigma(\mathbf{x}) d\mathbf{x} = \tau \right\}, \tag{2.2}$$

where σ_M and σ_m are constants and $\sigma_M > \sigma_m = 1$. It is well known that (2.1) has infinite number of eigenvalues $0 = \nu_0 < \nu_1 \le \nu_2 \le \nu_3 \le \cdots$ and the variational formula for the first nonzero eigenvalue λ is given by

$$\lambda = \nu_1(\sigma) = \min_{v \in \mathcal{S}} \frac{\int_\Omega \sigma(\mathbf{x}) |\nabla v(\mathbf{x})|^2 d\mathbf{x}}{\int_\Omega v(\mathbf{x})^2 dx}, \tag{2.3}$$

where the space $\mathcal{S} = \{v | v \in H^1(\Omega), v \ne 0, \int_\Omega v d\mathbf{x} = 0\}$. Our objective is to find

$$\min_D \lambda(D) \quad \text{such that} \quad \frac{|D|}{|\Omega|} = \gamma, \tag{2.4}$$

where γ is a given constant.

2.1. One-dimensional analytical result. In this section, we show the monotone increasing properties of λ in γ and σ_M. In one dimension, the optimal distribution of the material which has the minimal first nonzero eigenvalue is to have high conductivity material placed evenly at two ends of the boundary under the assumption that the region that has lower conductivity is simply connected.

LEMMA 1. *Consider the one-dimensional problem on $\Omega = [0, 1]$ and $D = [0, c] \cup [c + e, 1]$ where $c > 0$ and $e = 1 - \gamma > 0$ are given positive constants. The governing equation satisfies*

$$\begin{cases} (\sigma(x) u')' + \lambda u = 0, \\ \sigma(0) u'(0) = \sigma(1) u'(1) = 0, \end{cases} \tag{2.5}$$

with

$$\sigma(x) = \begin{cases} \sigma_M = b^2 & \text{if} \quad 0 \le x \le c, \\ \sigma_m = a^2 = 1 & \text{if} \quad c < x < c+e, \\ \sigma_M = b^2 & \text{if} \quad c+e \le x \le 1. \end{cases}$$

Denote the first nonzero eigenvalue $\lambda = k^2$. Then λ is a monotone increasing function in $\gamma = 1-e$ and σ_M. Furthermore, $ke < \pi$.

Proof. From the variational formula,

$$\lambda = k^2 = \inf_{v\in\mathcal{S}} \frac{\int_\Omega \sigma |v'|^2 dx}{\int_\Omega |v|^2 dx},$$

it is clear that λ is a monotone increasing function in $\gamma = 1-e$ and in σ_M. Furthermore, we know that

$$\lambda = k^2 = \inf_{v\in\mathcal{S}} \frac{\int_\Omega \sigma |v'|^2 dx}{\int_\Omega |v|^2 dx} < \inf_{v\in\mathcal{S}\cap A} \frac{\int_\Omega |v'|^2 dx}{\int_\Omega |v|^2 dx} = \left(\frac{\pi}{e}\right)^2,$$

where A is the class of functions v such that $v(x)$ is constant when $0 \le x \le c$ or $c+e \le x \le 1$. Thus we have $ke < \pi$. ∎

LEMMA 2. *Consider the one-dimensional problem* (2.5). *Use k to denote the square root of the eigenvalue and define new parameters α, β, and d as follows:*

$$\alpha = ke,\ \beta = \frac{k}{b}(1-e),\ d = \frac{k}{b}(1-2c-e).$$

Then these parameters satisfy the equation

$$\frac{b^2+1}{2}\sin\alpha\cos\beta - \frac{b^2-1}{2}\sin\alpha\cos d + b\cos\alpha\sin\beta = 0. \tag{2.6}$$

Proof. The solution of (2.5) can be written as

$$u(x) = \begin{cases} C_1\cos\left(\frac{k}{b}(x-c)\right) + C_2\sin\left(\frac{k}{b}(x-c)\right) & \text{if} \quad 0 \le x < c, \\ C_3\cos\left(k(x-c)\right) + C_4\sin\left(k(x-c)\right) & \text{if} \quad c \le x \le c+e, \\ C_5\cos\left(\frac{k}{b}(x-(c+e))\right) + C_6\sin\left(\frac{k}{b}(x-(c+e))\right) & \text{if} \quad c+e < x \le 1, \end{cases}$$

with the boundary conditions and the following conditions:

$$\lim_{x\to c^-} u(x) = \lim_{x\to c^+} u(x), \quad \sigma(x)u'(x)\Big|_{c^-}^{c^+} = 0,$$

$$\lim_{x\to (c+e)^-} u(x) = \lim_{x\to (c+e)^+} u(x), \quad \sigma(x)u'(x)\Big|_{(c+e)^-}^{(c+e)^+} = 0.$$

We then have

$$\begin{bmatrix} \sin\left(\frac{k}{b}c\right) & \cos\left(\frac{k}{b}c\right) & 0 & 0 & 0 & 0 \\ 1 & 0 & -1 & 0 & 0 & 0 \\ 0 & b & 0 & -1 & 0 & 0 \\ 0 & 0 & \cos(ke) & \sin(ke) & -1 & 0 \\ 0 & 0 & -\sin(ke) & \cos(ke) & 0 & -b \\ 0 & 0 & 0 & 0 & -\sin\left(\frac{k}{b}(1-c-e)\right) & \cos\left(\frac{k}{b}(1-c-e)\right) \end{bmatrix} \begin{bmatrix} C_1 \\ C_2 \\ C_3 \\ C_4 \\ C_5 \\ C_6 \end{bmatrix} = \begin{bmatrix} 0 \\ 0 \\ 0 \\ 0 \\ 0 \\ 0 \end{bmatrix}.$$

Denote the determinant of the matrix by f. In order to have nontrivial solutions, f needs to be zero. This leads to

$$f(b,c,e,k) = -\sin(ke)\left[b^2 \sin\left(\frac{k}{b}(1-e-c)\right)\sin\left(\frac{kc}{b}\right) - \cos\left(\frac{k}{b}(1-e-c)\right)\cos\left(\frac{kc}{b}\right)\right] + b\cos(ke)\left[\sin\left(\frac{k}{b}(1-e)\right)\right] = 0.$$

After applying change of variables $\alpha = ke,\ \beta = \frac{k}{b}(1-e),\ d = \frac{k}{b}(1-2c-e)$ and using trigonometric identities to simplify the expression, we have

$$f(b,\alpha,\beta,d) = \frac{b^2+1}{2}\sin\alpha\cos\beta - \frac{b^2-1}{2}\sin\alpha\cos d + b\cos\alpha\sin\beta = 0. \tag{2.7}$$ ∎

THEOREM 3. *Consider the one-dimensional problem* (2.5) *for any given fixed* b *and* e*. The* $\sigma(x)$ *which minimizes* λ *must have* $c = \frac{1-e}{2}$*.*

Proof. The statement of this theorem requires us to prove that $k(c)$ gets its minimum at $c = \frac{1-e}{2}$. To show this, we use the chain rule to express the derivative of k with respect to c.

$$\frac{\partial k}{\partial c} = -\left(\frac{\partial f}{\partial c}\right) / \left(\frac{\partial f}{\partial k}\right).$$

From Lemma 2, we can calculate directly that

$$\frac{\partial f}{\partial c} = -\frac{2k}{b}\frac{\partial f}{\partial d} = -\left(kb - \frac{k}{b}\right)\sin\alpha\sin d.$$

From Lemma 1, we know that $\alpha = ke < \pi$. This implies

$$\frac{\partial f}{\partial c} = \begin{cases} >0 & \text{if} \quad d<0, \\ =0 & \text{if} \quad d=0, \\ <0 & \text{if} \quad d>0. \end{cases} \tag{2.8}$$

Next we use Lemma 2 to calculate the expression for $\frac{\partial f}{\partial k}$ as

$$\begin{aligned} k\frac{\partial f}{\partial k} &= \left(\frac{\alpha}{2}(b^2+1) + b\beta\right)\cos\alpha\cos\beta - \frac{\alpha}{2}(b^2-1)\cos\alpha\cos d \\ &\quad + \frac{d}{2}(b^2-1)\sin\alpha\sin d - \left(\frac{\beta}{2}(b^2+1) + b\alpha\right)\sin\alpha\sin\beta. \end{aligned} \tag{2.9}$$

Since $f = 0$, from (2.6) we have

$$\cos\alpha = -\frac{b^2+1}{2b\sin\beta}\sin\alpha\cos\beta + \frac{b^2-1}{2b\sin\beta}\sin\alpha\cos d.$$

Substitute this expression into (2.9) and simplify to get

$$\begin{aligned} k\frac{\partial f}{\partial k} = \frac{\sin\alpha}{\sin\beta}\Bigg[&\frac{b^2-1}{2}(\beta\cos\beta\cos d + d\sin\beta\sin d) \\ &- \alpha b\sin^2\beta - \frac{b^2+1}{2}\beta - \frac{\alpha}{b}\left(\frac{b^2+1}{2}\cos\beta - \frac{b^2-1}{2}\cos d\right)^2\Bigg]. \end{aligned} \tag{2.10}$$

Denote

$$g(\beta, d) = \beta \cos\beta \cos d + d \sin\beta \sin d. \tag{2.11}$$

Notice that $g(\beta, d)$ is an even function in d. We just need to discuss the case when $0 \le d < \beta < \pi$. In this case, we have

$$g(\beta, d) < \beta \cos\beta \cos d + \beta \sin\beta \sin d = \beta \cos(\beta - d) < \beta.$$

Equation (2.10) then gives us

$$k\frac{\partial f}{\partial k} < \frac{\sin\alpha}{\sin\beta}\left[\frac{b^2-1}{2}\beta - \alpha b \sin^2\beta - \frac{b^2+1}{2}\beta\right] \tag{2.12}$$

$$= -\frac{\sin\alpha}{\sin\beta}\left[\beta + \alpha b \sin^2\beta\right] \le 0. \tag{2.13}$$

Together with inequality (2.8), we know that

$$\frac{\partial k}{\partial c} = -\frac{\frac{\partial f}{\partial c}}{\frac{\partial f}{\partial k}} = \begin{cases} > 0 & \text{if} \quad c > \frac{1-e}{2}, \\ = 0 & \text{if} \quad c = \frac{1-e}{2}, \\ < 0 & \text{if} \quad c < \frac{1-e}{2}. \end{cases}$$ □

2.2. Two-dimensional results on a rectangular domain. In this section, we will prove that the strip configuration of conductivity parallel to short edges is a local minimizer on the rectangular domain under a certain assumption. The Fourier series expressions of the eigenfunctions are obtained and the equations that determine eigenvalues are derived. A thorough comparison of eigenvalues to determine the minimal nonzero eigenvalue allows us to show that the one corresponding to the strip configuration is indeed the minimizer.

LEMMA 4. *When $\sigma_M > \sigma_m$, the first eigenfunction of (2.1) on a rectangular domain $[-\frac{1}{2}, \frac{1}{2}] \times [0, L]$ with $\bar{\sigma}(x, y) = \sigma_M \chi_{([-\frac{1}{2}, -d] \cup [d, \frac{1}{2}]) \times [0,L]} + \sigma_m \chi_{(-d,d) \times [0,L]}$, $L \le 1$, depends only on x.*

Proof. (i) The equation with the given $\bar{\sigma}$ can be written in piecewise form as follows:

$$\begin{aligned} -\nabla \cdot (\sigma_M \nabla u_1) &= \lambda u_1, \quad -\frac{1}{2} < x \le -d, 0 < y < L, \\ -\nabla \cdot (\sigma_m \nabla u_2) &= \lambda u_2, \quad -d < x < d, 0 < y < L, \\ -\nabla \cdot (\sigma_M \nabla u_1) &= \lambda u_1, \quad d \le x < \frac{1}{2}, 0 < y < L. \end{aligned}$$

The general solutions can be written in the following form by using separation of variables:

$$\begin{aligned} u_1 &= \sum_n E_n \cos\left(A\left(x + \frac{1}{2}\right)\right) \cos\left(\frac{n\pi}{L}y\right), \quad n \text{ is an integer}, \\ u_2 &= \sum_n \left(F_n \cos(Bx) + G_n \sin(Bx)\right) \cos\left(\frac{n\pi}{L}y\right), \\ u_3 &= \sum_n H_n \cos\left(A\left(\frac{1}{2} - x\right)\right) \cos\left(\frac{n\pi}{L}y\right), \end{aligned}$$

where $A = \sqrt{\frac{\lambda}{\sigma_M} - \left(\frac{n\pi}{L}\right)^2}$ and $B = \sqrt{\frac{\lambda}{\sigma_m} - \left(\frac{n\pi}{L}\right)^2}$. The boundary conditions and smoothness conditions of the eigenfunction lead to a system of equations

$$\begin{pmatrix} \cos\left(A\left(\frac{1}{2}-d\right)\right) & -\cos(Bd) & \sin(Bd) & 0 \\ -\sigma_M A\sin\left(A\left(\frac{1}{2}-d\right)\right) & -\sigma_m B\sin(Bd) & -\sigma_m B\cos(Bd) & 0 \\ 0 & -\cos(Bd) & -\sin(Bd) & \cos\left(A\left(\frac{1}{2}-d\right)\right) \\ 0 & \sigma_m B\sin(Bd) & -\sigma_m B\cos(Bd) & \sigma_M A\sin\left(A\left(\frac{1}{2}-d\right)\right) \end{pmatrix} \begin{pmatrix} E_m \\ F_m \\ G_m \\ H_m \end{pmatrix} = \begin{pmatrix} 0 \\ 0 \\ 0 \\ 0 \end{pmatrix}.$$

In order to have nontrivial solutions, the determinant of the matrix should be zero, i.e.,

$$\left(\left(\frac{A}{B}\right)^2 \tan^2(p) - \left(\frac{\sigma_m}{\sigma_M}\right)^2\right)\tan(2q) - 2\frac{A\sigma_m}{B\sigma_M}\tan(p) = 0,$$

where $p = \frac{1-2d}{2}A$ and $q = Bd$. Solving this quadratic equation with respect to $\tan(p)$, we have either

$$\frac{A\sigma_M}{B\sigma_m}\tan(p)\tan(q) = 1 \tag{2.14}$$

or

$$\frac{A\sigma_M}{B\sigma_m}\tan(p)\cot(q) = -1. \tag{2.15}$$

(ii) We show that the smallest positive eigenvalues for λ of (2.14) and (2.15) are achieved when $n = 0$ and $n = 1$, respectively. Instead of comparing eigenvalues for integers n only, we establish the monotone increasing of λ with respect to n. Note that if A or B is not real, which means that $\frac{\lambda}{\sigma_M} < \left(\frac{n\pi}{L}\right)^2$ or $\frac{\lambda}{\sigma_m} < \left(\frac{n\pi}{L}\right)^2$, then A or B is pure imaginary. Since $A\tan(p) = (iA)\tanh(ip)$ (or similarly, $B\cot(q) = -(iB)\coth(iq)$), the expressions are real no matter whether A and B are real or not. Thus we can do the following calculation formally to derive the results.

Equation (2.14) is equivalent to

$$F_1(\lambda, t) = 2\sigma_M d f(p) + (1-2d)\sigma_m g(q) = 0,$$

where $f(x) = x\tan(x)$ and $g(x) = -x\cot(x)$. Denote $t = (\frac{n\pi}{L})^2$. By using the implicit differentiation formula, we have

$$\frac{\partial\lambda}{\partial t} = -\frac{\frac{\partial F_1}{\partial t}}{\frac{\partial F_1}{\partial\lambda}} = -\frac{2\sigma_M d\frac{df}{dp}\frac{\partial p}{\partial t} + (1-2d)\sigma_m\frac{dg}{dq}\frac{\partial q}{\partial t}}{2\sigma_M d\frac{df}{dp}\frac{\partial p}{\partial\lambda} + (1-2d)\sigma_m\frac{dg}{dq}\frac{\partial q}{\partial\lambda}} = \frac{\frac{df}{dp}\frac{(1-2d)}{4\sigma_M p} + \frac{dg}{dq}\frac{d}{2\sigma_m q}}{\frac{df}{dp}\frac{(1-2d)}{4p} + \frac{dg}{dq}\frac{d}{2q}} > 0$$

because $f'(x) = \tan x + x\sec^2 x > 0$ for $x > 0$ and $g'(x) = -\cot x + x\csc^2 x > 0$ for $x > 0$ whenever the derivatives exist. Thus λ is increasingly dependent on n and the first nonzero eigenvalue is given by $n = 0$.

Equation (2.15) is equivalent to

$$F_2(\lambda, t) = 2\sigma_M d f(p) + (1-2d)\sigma_m f(q) = 0.$$

By using the implicit differentiation formula, we have

$$\frac{\partial\lambda}{\partial t} = -\frac{\frac{\partial F_2}{\partial t}}{\frac{\partial F_2}{\partial\lambda}} = -\frac{2\sigma_M d\frac{df}{dp}\frac{\partial p}{\partial t} + (1-2d)\sigma_m\frac{df}{dq}\frac{\partial q}{\partial t}}{2\sigma_M d\frac{df}{dp}\frac{\partial p}{\partial\lambda} + (1-2d)\sigma_m\frac{df}{dq}\frac{\partial q}{\partial\lambda}} = \frac{\frac{df}{dp}\frac{(1-2d)}{4\sigma_M p} + \frac{df}{dq}\frac{d}{2\sigma_m q}}{\frac{df}{dp}\frac{(1-2d)}{4p} + \frac{df}{dq}\frac{d}{2q}} > 0$$

due to $f'(x) > 0$ for $x > 0$ whenever the derivative exists. Since (2.15) has no roots when $n = 0$, the first nonzero eigenvalue is given by $n = 1$.

(iii) Denote the smallest root of (2.14) with $n = 0$ by $\check{\lambda}$ and the smallest root of (2.15) with $n = 1$ by $\hat{\lambda}$. We now show $\check{\lambda} < \hat{\lambda}$. Noticing that $\hat{\lambda} = \hat{\lambda}(\sigma_m, \sigma_M, d, L)$ is a decreasing function in L as $\frac{\partial\lambda}{\partial L} = \frac{\partial\lambda}{\partial t}\frac{\partial t}{\partial L} < 0$ and $\check{\lambda} = \check{\lambda}(\sigma_m, \sigma_M, d)$ is independent of L, the statement is true if we can demonstrate that $\hat{\lambda}(\sigma_m, \sigma_M, d, 1) > \check{\lambda}(\sigma_m, \sigma_M, d)$.

Without loss of generality, we choose $\sigma_m = 1$ and $\sigma_M > \sigma_m = 1$. We compare the first root for equation

$$F_1(\check{\lambda}, \sigma_M) = \sqrt{\sigma_M}\tan\left(\frac{1-2d}{2}\sqrt{\frac{\check{\lambda}}{\sigma_M}}\right) - \cot(d\sqrt{\check{\lambda}}) = 2\sigma_M d f(p_0) + (1-2d)g(q_0) = 0$$

and

$$\begin{aligned} F_2(\hat{\lambda}, \sigma_M) &= \sqrt{\sigma_M}\tan\left(\frac{1-2d}{2}\sqrt{\frac{\hat{\lambda}}{\sigma_M} - \pi^2}\right) + \sqrt{\hat{\lambda} - \pi^2}\tan\left(d\sqrt{\hat{\lambda} - \pi^2}\right) \\ &= 2\sigma_M d f(p_1) + (1-2d)f(q_1) = 0, \end{aligned}$$

where $p_0 = \frac{1-2d}{2}\sqrt{\frac{\check{\lambda}}{\sigma_M}}$, $q_0 = d\sqrt{\check{\lambda}}$, $p_1 = \frac{1-2d}{2}\sqrt{\frac{\hat{\lambda}}{\sigma_M} - \pi^2}$, and $q_1 = d\sqrt{\hat{\lambda} - \pi^2}$ are the numbers when p and q take value at $n = 0$ and $n = 1$, respectively.

Note that $\check{\lambda}, \hat{\lambda} \in (\pi^2, \sigma_M\pi^2)$, and when $\sigma_M = 1$, $F_1 = 0$, and $F_2 = 0$ have common solutions $\check{\lambda} = \hat{\lambda} = \pi^2$, we compare the growth rate of $\check{\lambda}$ and $\hat{\lambda}$ with respect to σ_M. From the implicit formula, we have

(2.16)
$$\frac{\partial\check{\lambda}}{\partial\sigma_M} = -\frac{\frac{\partial F_1}{\partial\sigma_M}}{\frac{\partial F_1}{\partial\check{\lambda}}} = -\frac{2\sigma_M d f'(p_0)\frac{\partial p_0}{\partial\sigma_M}}{2\sigma_M d f'(p_0)\frac{\partial p_0}{\partial\check{\lambda}} + (1-2d)g'(q_0)\frac{\partial q_0}{\partial\check{\lambda}}} = \frac{2\sigma_M d f'(p_0)\frac{p_0}{\sigma_M}}{2\sigma_M d f'(p_0)\frac{p_0}{\check{\lambda}} + (1-2d)g'(q_0)\frac{q_0}{\check{\lambda}}},$$

(2.17)
$$\frac{\partial\hat{\lambda}}{\partial\sigma_M} = -\frac{\frac{\partial F_2}{\partial\sigma_M}}{\frac{\partial F_2}{\partial\hat{\lambda}}} = -\frac{2\sigma_M d f'(p_1)\frac{\partial p_1}{\partial\sigma_M}}{2\sigma_M d f'(p_1)\frac{\partial p_1}{\partial\hat{\lambda}} + (1-2d)f'(q_1)\frac{\partial q_1}{\partial\hat{\lambda}}} = \frac{2\sigma_M d f'(p_1)\frac{p_1}{\sigma_M}}{2\sigma_M d f'(p_1)\frac{p_1}{\hat{\lambda}} + (1-2d)f'(q_1)\frac{q_1}{\hat{\lambda}}}.$$

Next we compare $\frac{q_0 g'(q_0)}{p_0 f'(p_0)}$ and $\frac{q_1 f'(q_1)}{p_1 f'(p_1)}$:

$$\begin{aligned} \frac{q_0 g'(q_0)}{p_0 f'(p_0)} &= \frac{q_0(-\cot q_0 + q_0 + q_0\cot^2 q_0)}{p_0(\tan p_0 + p_0 + p_0\tan^2 p_0)} = \frac{q_0^2 + g(q_0) + g(q_0)^2}{p_0^2 + f(p_0) + f(p_0)^2} \\ &= \frac{\frac{4\sigma_M d^2}{(1-2d)^2}p_0^2 - \frac{2\sigma_M d}{1-2d}f(p_0) + (\frac{2\sigma_M d}{1-2d})^2 f(p_0)^2}{p_0^2 + f(p_0) + f(p_0)^2}, \end{aligned}$$

$$\frac{q_1 f'(q_1)}{p_1 f'(p_1)} = \frac{q_1^2 + f(q_1) + f(q_1)^2}{p_1^2 + f(p_1) + f(p_1)^2} = \frac{\frac{4\sigma_M d^2}{(1-2d)^2}p_1^2 - \frac{2\sigma_M d}{1-2d}f(p_1) + (\frac{2\sigma_M d}{1-2d})^2 f(p_1)^2 + d^2(\sigma_M - 1)\pi^2}{p_1^2 + f(p_1) + f(p_1)^2}.$$

Let $h_1(x) = \frac{\frac{4\sigma_M d^2}{(1-2d)^2}x^2 - \frac{2\sigma_M d}{1-2d}f(x) + (\frac{2\sigma_M d}{1-2d})^2 f(x)^2}{x^2 + f(x) + f(x)^2}$; this function is increasing on $[0, \frac{\pi}{2}]$. Also define $h_2(x) = h_1(ix)$, and $h_2(x)$ is decreasing on $[0, \frac{\pi}{2}]$. Using the fact that p_0

is real and p_1 is pure imaginary, we have

$$\begin{aligned}\frac{q_0 g'(q_0)}{p_0 f'(p_0)} - \frac{q_1 f'(q_1)}{p_0 f'(p_1)} &= h_1(p_0) - h_2(ip_1) - \frac{d^2(\sigma_M - 1)\pi^2}{p_1^2 + f(p_1) + f(p_1)^2} \\ &> h_1(0) - h_2(0) + 0 \\ &= 0.\end{aligned}$$

Since $\frac{q_0 g'(q_0)}{p_0 f'(p_0)} > \frac{q_1 f'(q_1)}{p_1 f'(p_1)}$ and $p_1 f'(p_1) < 0$, we have

$$\frac{2\sigma_M d f'(p_0) p_0}{2\sigma_M d f'(p_0) p_0 + (1-2d) g'(q_0) q_0} < \frac{2\sigma_M d f'(p_1) p_1}{2\sigma_M d f'(p_1) p_1 + (1-2d) f'(q_1) q_1}. \tag{2.18}$$

Comparing (2.18) with (2.16) and (2.17) derives $\frac{\partial \ln \check{\lambda}}{\partial \ln \sigma_M} < \frac{\partial \ln \hat{\lambda}}{\partial \ln \sigma_M}$, which means that the growth rate for $\check{\lambda}$ is smaller than that of $\hat{\lambda}$ with respect to σ_M. Thus $\check{\lambda} < \hat{\lambda}$ for $\sigma_M > 1$. ∎

THEOREM 5. *Denote* $\bar{\sigma}(x) = \sigma_M \chi_{([-\frac{1}{2}, -d] \cup [d, \frac{1}{2}]) \times [0,L]} + \sigma_m \chi_{(-d,d)\times[0,L]}$ *and* $(\lambda(\sigma), u)$ *as the first nonzero eigenpair of* (2.1) *with the slightly perturbed conductivity* $\sigma(x,y) = \bar{\sigma}(x) + \epsilon\sigma_1(x,y)$ *on* $\Omega = [-\frac{1}{2}, \frac{1}{2}] \times [0, L]$, $L \le 1$, *which satisfies*

$$\int_\Omega \sigma_1(x,y)dxdy = 0 \tag{2.19}$$

and

$$\begin{cases} \sigma_1(x,y) \ge 0 & \text{if} \quad -d < x < d, \\ \sigma_1(x,y) \le 0 & \text{if} \quad -\frac{1}{2} \le x \le -d \text{ or } d \le x \le \frac{1}{2}, \end{cases} \tag{2.20}$$

where $\epsilon > 0$ *is much smaller than* 1. *Then*

$$\lambda(\sigma(x,y)) > \lambda(\bar{\sigma}(x)). \tag{2.21}$$

Proof. Note that the slightly perturbed conductivity $\sigma(x,y) = \bar{\sigma}(x) + \epsilon\sigma_1(x,y)$ remains in the class of functions defined by

$$A^\star_{\sigma_m,\sigma_M,\tau} := \left\{\sigma \in L^\infty(\Omega); 0 < \sigma_m \le \sigma(\mathbf{x}) \le \sigma_M \text{ a.e. in } \Omega; \int_\Omega \sigma(\mathbf{x})d\mathbf{x} = \tau\right\},$$

where $\tau = L\left((1-2d)\,\sigma_M + 2d\sigma_m\right)$ is given. We can write the first eigenpair (λ, u) in asymptotic form as follows:

$$\lambda = \lambda_0 + \epsilon\lambda_1 + \epsilon^2\lambda_2 + \cdots,$$

$$u(x,y) = u_0(x,y) + \epsilon u_1(x,y) + \epsilon^2 u_2(x,y) + \cdots.$$

Without loss of generality, we assume u is normalized, i.e., $\int_\Omega u^2 dxdy = 1$. Substituting the asymptotic forms of u and λ into this normalization equation, we have orthogonality of u_0 and u_1,

$$\int_\Omega u_0(x,y)u_1(x,y)dxdy = 0.$$

Substituting the asymptotic forms of λ and u into (2.1) and collecting the leading order terms yields

$$\begin{cases} -\frac{\partial}{\partial x}\left(\bar{\sigma}(x)\frac{\partial}{\partial x}u_0(x,y)\right) - \frac{\partial}{\partial y}\left(\bar{\sigma}(x)\frac{\partial}{\partial y}u_0(x,y)\right) = \lambda_0 u_0(x,y) \quad \text{in } \Omega, \\ \bar{\sigma}(x)\dfrac{\partial u_0(x)}{\partial n} = 0 \quad \text{for } x \in \partial\Omega. \end{cases} \tag{2.22}$$

Thus (λ_0, u_0) is the first eigenpair of the equation with $\sigma(x,y) = \bar{\sigma}(x)$, so $u_0(x,y) = u_0(x)$ due to Lemma 4. Next we consider the ϵ order term,

$$\nabla \cdot (\sigma_1 \nabla u_0) + \nabla \cdot (\bar{\sigma}(x)\nabla u_1) = -\lambda_0 u_1 - \lambda_0 u_0.$$

Multiply by $u_0(x)$ and integrate over Ω to get

$$\int_\Omega u_0(x)\left(\nabla \cdot (\sigma_1 \nabla u_0) + \nabla \cdot (\bar{\sigma}(x)\nabla u_1) + \lambda_0 u_1 + \lambda_1 u_0\right) dxdy = 0.$$

After doing integration by parts and using the orthogonality properties, the equation becomes

$$\lambda_1 = \int_\Omega \sigma_1 u_0'(x)^2 dxdy + \int_\Omega \bar{\sigma}(x)u_0'(x)\frac{\partial u_1(x,y)}{\partial x} dxdy.$$

The second term on the right-hand side is 0 due to integration by parts and (2.22), so we have the expression

$$\lambda_1 = \int_{-\frac{1}{2}}^{\frac{1}{2}} \left(\int_0^L \sigma_1(x,y)dy\right) u_0'(x)^2 dx.$$

Since $u_0(x)$ is the first eigenfunction for (2.22) with Neumann boundary condition, we know that

$$\min_{x\in(-d,d)} u_0'(x)^2 \geq \max_{x\in[-\frac{1}{2},-d]\cup[d,\frac{1}{2}]} u_0'(x)^2.$$

Along with (2.19) and (2.20), we can prove that

$$\begin{aligned} \lambda_1 &= \int_{-d}^{d}\int_0^L \sigma_1(x,y)u_0^{'}(x)^2 dydx + \int_{[-\frac{1}{2},-d]\cup[d,\frac{1}{2}]}\int_0^L \sigma_1(x,y)u_0^{'}(x)^2 dydx \\ &\geq \int_{-d}^{d}\int_0^L \sigma_1(x,y)\min_{x\in[-d,d]} u_0^{'}(x)^2 dydx + \int_{[-\frac{1}{2},-d]\cup[d,\frac{1}{2}]}\int_0^L \sigma_1(x,y)\max_{x\in[-\frac{1}{2},-d]\cup[d,\frac{1}{2}]} u_0^{'}(x)^2 dydx \\ &\geq \int_{-d}^{d}\int_0^L \sigma_1(x,y)\min_{x\in[-d,d]} u_0^{'}(x)^2 dydx + \int_{[-\frac{1}{2},-d]\cup[d,\frac{1}{2}]}\int_0^L \sigma_1(x,y)\min_{x\in[-d,d]} u_0^{'}(x)^2 dydx = 0, \end{aligned}$$

and the equal sign holds if and only if $u_0^{'}(x) = 0$, which is impossible. Thus we proved that

$$\lambda(\sigma(x,y)) > \lambda(\bar{\sigma}(x))$$

for sufficiently small ϵ. ∎

2.3. Rearrangement. There is a simple way to find a decreasing sequence of λ providing an initial conductivity $\sigma = \sigma^{(0)}$ whose corresponding first eigenpair is $(\lambda^{(0)}, u^{(0)})$. At each step, the rearrangement method is used to find new conductivity which generates a smaller first nonzero eigenvalue as described in the following. At the ith step, find the eigenpair $(\lambda^{(i)}, u^{(i)})$ of $\sigma^{(i)}$ and choose $\sigma^{(i+1)}$ satisfying

$$\sigma^{(i+1)} = \arg \min_{\sigma \in A_{\sigma_m,\sigma_M,\tau}} \int_\Omega \sigma |\nabla u_i|^2 dx,$$

where $\tau = (\sigma_M \gamma + \sigma_m(1-\gamma))|\Omega|$. Denote $D^{(i)} = \{x|\sigma^{(i)}(x) = \sigma_M\}$ and $(D^{(i)})^c = \{x|\sigma^{(i)}(x) = \sigma_m\}$. To obtain such $\sigma^{(i+1)}$, we can choose $D^{(i+1)}$ and $(D^{(i+1)})^c$ such that

$$\min_{x \in (D^{(i+1)})^c} |\nabla u^{(i)}| \geq \max_{x \in D^{(i+1)}} |\nabla u^{(i)}|$$

and

$$|D^{(i+1)}| = \gamma |\Omega|.$$

This means that $D^{(i+1)} = \{x \in \Omega : |\nabla u^{(i)}| \leq t\}$, where

$$t = \inf\{s : |\{x \in \Omega : |\nabla u^{(i)}| \leq s\}| \geq \gamma |\Omega|\}. \tag{2.23}$$

Note that $(D^{(i)})^c \backslash (D^{(i+1)})^c = D^{(i+1)} \backslash D^{(i)}$ and $(D^{(i+1)})^c \backslash D^{(i)} = (D^{(i)})^c \backslash (D^{i+1})$. Thus we can prove that

$$\int_\Omega \sigma^{(i+1)} (\nabla u^{(i)})^2 dx \leq \int_\Omega \sigma^{(i)} (\nabla u^{(i)})^2 dx.$$

After choosing $\sigma^{(i+1)}$, we calculate the first eigenpair $(\lambda^{(i+1)}, u^{(i+1)})$ using $\sigma = \sigma^{(i+1)}$. Then we have the inequality

$$\lambda^{(i+1)} = \min_{v \in \mathcal{S}} \frac{\int_\Omega \sigma^{(i+1)} (\nabla v(x))^2 dx}{\int_\Omega v(x)^2 dx} = \frac{\int_\Omega \sigma^{(i+1)} (\nabla u^{(i+1)})^2 dx}{\int_\Omega (u^{(i+1)})^2 dx}$$
$$\leq \frac{\int_\Omega \sigma^{(i+1)} (\nabla u^{(i)})^2 dx}{\int_\Omega (u^{(i)})^2 dx} \leq \frac{\int_\Omega \sigma^{(i)} (\nabla u^{i})^2 dx}{\int_\Omega (u^{i})^2 dx} = \lambda^{(i)}.$$

This process provides us a decreasing sequence of $\lambda^{(i)}$. Repeat this process until $\sigma^{(i+1)} = \sigma^{(i)}$ and $\lambda^{(i+1)} = \lambda^{(i)}$ numerically. This provides us an estimated optimal distribution of σ and an estimated minimal eigenvalue λ. In Algorithm 2.1, we summarize the steps of the rearrangement approach.

Algorithm 2.1 Minimization algorithm

Given $\sigma_m, \sigma_M, \Omega, D$, and γ, choose an initial conductivity $\sigma = \sigma^{(0)} = \sigma_M \chi_{D^0} + \sigma_m \chi_{\Omega \backslash D^0}$.
1. Set $i = 0$.
2. Compute $u^{(i)}$ and $\lambda^{(i)}$ of (2.1) by using a finite element method with $\sigma = \sigma^{(i)}$.
3. Compute $D^{(i+1)}$ to satisfy (2.23) and assign $\sigma^{(i+1)} = \sigma_M \chi_{D^{(i+1)}} + \sigma_m \chi_{\Omega \backslash D^{(i+1)}}$.
4. If $\sigma^{(i+1)} = \sigma^{(i)}$, stop the algorithm. Otherwise set $i = i + 1$, go to step 2.

3. Numerical simulations. In this section, we show numerical results for the optimization problem (2.1)–(1.2) on different domains. For the forward problem, we perform a classical finite element method with linear elements and calculate the eigenvalues and eigenfunctions via Arnoldi's method. For the optimization problem, we use the rearrangement approach discussed in section 2.3. In this section we choose $\sigma_M = 1.1$ and $\sigma_m = 1$ for all numerical simulations.

Table 1
The numerical solutions and the convergence rate of λ on $[0,1]$ with $\sigma = 1 + 0.1\chi_{[0,0.1]\cup[0.9,1]}$. A second order accuracy is obtained.

Mesh size	$h = 1/200$	$h = 1/400$	$h = 1/800$	$h = 1/1600$	$h = 1/3200$
λ^h	9.881361	9.881213	9.881176	9.881167	9.881165
$\log_2 \lvert \frac{\lambda^h - \lambda^{h/2}}{\lambda^{h/2} - \lambda^{h/4}} \rvert$	2.000	2.000	2.001		

Table 2
The numerical solutions of λ on a square domain $[0,1]\times[0,1]$ for $\sigma = 1+0.1\chi_{([0,0.3]\cup[0.7,1])\times[0,1]}$ with Neumann boundary conditions and the convergence rate. A second order accuracy is obtained.

Mesh size	$h = 2^{-7}$	$h = 2^{-8}$	$h = 2^{-9}$	$h = 2^{-10}$	$h = 2^{-11}$
λ^h	10.144242	10.142524	10.142094	10.141986	10.141944
$\log_2 \lvert \frac{\lambda^h - \lambda^{h/2}}{\lambda^{h/2} - \lambda^{h/4}} \rvert$	1.999	2.000	2.000		

3.1. Accuracy test. In this subsection we test the accuracy of the forward solver on a one-dimensional interval and two-dimensional domains. First we consider the eigenvalue problem (2.1) on $[0,1]$. We compute λ with $\sigma = 1 + 0.1\chi_{[0,0.1]\cup[0.9,1]}$, and the results for various mesh sizes h are shown in Table 1. The order of convergence is estimated via the base-2 logarithm of ratio of consecutive differences between three solutions obtained by mesh sizes h, $\frac{h}{2}$, and $\frac{h}{4}$. A second order accuracy is observed.

To test the order of accuracy on two-dimensional domain, we choose the domain as $\Omega = [0,1] \times [0,1]$ and $\sigma = 1 + 0.1\chi_{([0,0.3]\cup[0.7,1])\times[0,1]}$. The eigenvalue for various mesh sizes h are shown in Table 2, and the order of convergence is estimated via the base-2 logarithm of ratio of consecutive differences between three solutions obtained by mesh sizes h, $\frac{h}{2}$, and $\frac{h}{4}$. A second order accuracy is also observed.

3.2. Minimization of $\boldsymbol{\lambda}$ on $\mathbf{[0,1]}$. Now we apply the rearrangement algorithm to minimize the eigenvalue on the one-dimensional interval $[0,1]$. The initial guess of the conductivity function is $\sigma = 1 + 0.1\chi_{([0,0.125]\cup[0.375,0.625]\cup[0.875,1])}$. We show its corresponding eigenfunction and the absolute value of its derivative in Figure 1. The eigenvalue is $\lambda_1 \approx 10.3376$. After one iteration of the rearrangement algorithm, the optimal conductivity with $\lambda \approx 9.9570$ is achieved in a $\sigma_M - \sigma_m - \sigma_M$ configuration.

3.3. A square domain. Starting from here we study the optimization problem on various two-dimensional domains. We first consider solving the optimization problem on a square domain $\Omega = [0,1] \times [0,1]$ in $\mathbb{R}^2$. In Figure 2, eigenfunctions, absolute values of gradients of eigenfunctions, and optimal conductivity distributions are shown with different parameters $\gamma = 0.2$, 0.6, and 0.9. We found that for all values of γ, the optimal $D = \{x|\sigma(x) = \sigma_M\}$ consists of two strips attached to the side of the square. The σ_m material lies in the middle of the domain, in between the σ_M material. Due to the symmetry in both x and y directions on a square domain, we expect that the minimizer is not unique. As expected, we observe that λ increases as γ increases. We have used different initial choices of σ, and part of the choices for the case $\gamma = 0.4$ are shown in Figure 3. For all these initial choices, the optimal σ will converge to the strip scenario.

3.4. Rectangular domains. Consider the eigenvalue problem (2.1) with $\gamma = 0.6$ on elongated rectangles $[0,1] \times [0,b]$ with $b = 0.5, 2/3, 3/2$, and 1.5. We vary the values of b in order to see how λ and the optimal σ vary with respect to b. The

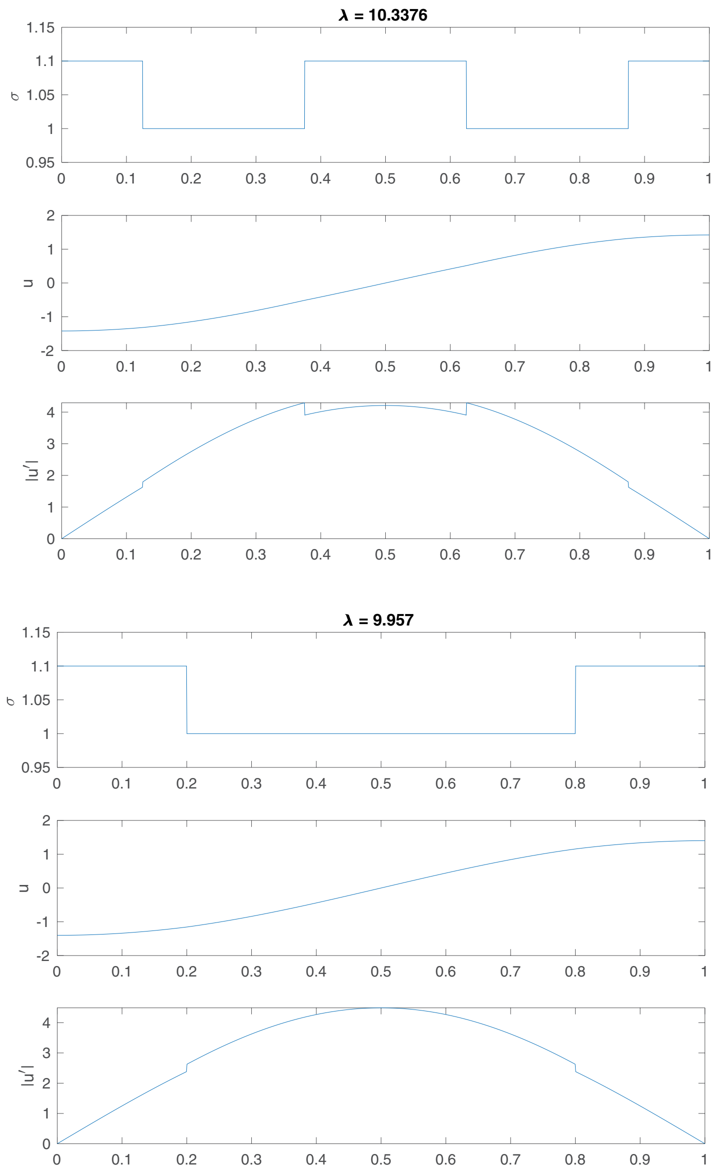

FIG. 1. *Minimizing λ by using the rearrangement algorithm on the interval* [0.1]. *Top: the initial guess of σ, the corresponding eigenfunction, and the absolute value of its derivative. Bottom: the optimal σ, the corresponding eigenfunction, and the absolute value of its derivative.*

optimal results are shown in Figure 4 with $b = 0.5, 2/3, 3/2$, and 1.5. From the first to third columns, eigenfunctions, absolute values of gradients of eigenfunctions, and the corresponding optimal conductivity distributions are shown. We observe that the optimal $D = \{x|\sigma(x) = \sigma_M\}$ consists of two strips attached to the shorter edges, while $D^c = \{x|\sigma(x) = \sigma_m\}$ consists of a strip in the middle of the rectangle. The results are consistent with those on an interval which have the σ_M material placed on both ends symmetrically and the σ_m material placed in the middle. Figure 5 shows the dependence between the optimal eigenvalue λ and the length of shorter edges b

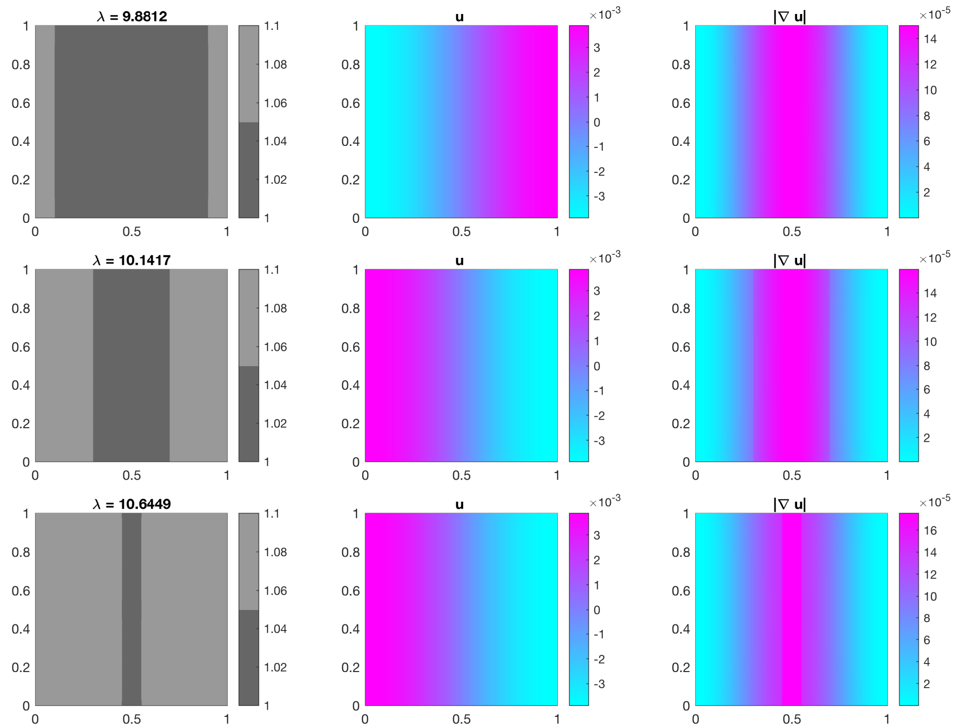

Fig. 2. *The optimal results on a square domain. From the left to right columns are shown the optimal conductivities σ, corresponding eigenfunctions, and absolute values of gradients of eigenfunctions with $\gamma = 0.2, 0.6,$ and 0.9 from the first row to the last row.*

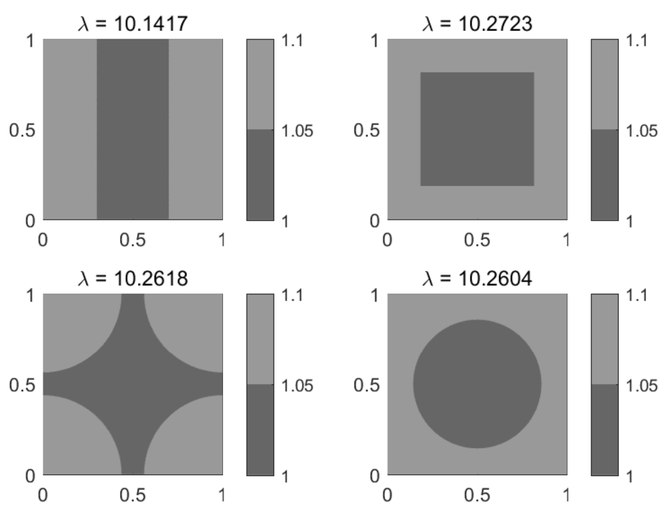

Fig. 3. *Different initial choices of σ with their corresponding eigenvalues for $\gamma = 0.6$.*

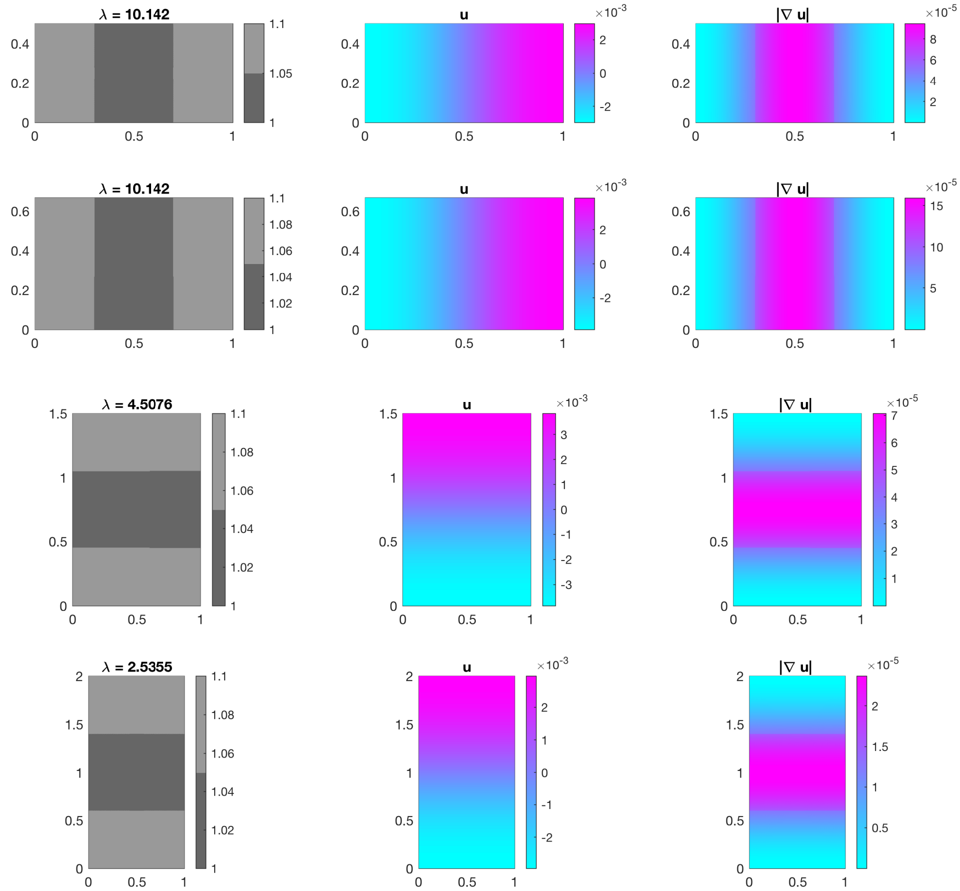

Fig. 4. *The optimal results on rectangular domains. From the left to right columns are shown the optimal conductivities σ, corresponding eigenfunctions, and absolute values of gradients of eigenfunctions with $\gamma = 0.6$ fixed. The ratio of edges from first to last rows are $\frac{1}{2}$, $\frac{2}{3}$, $\frac{3}{2}$, and 2.*

more directly with various choices of γ. When $b \leq 1$, the optimal conductivities σ on rectangular domains $[0,1] \times [0,b]$ do not depend on y and are similar to the optimal solution on the unit interval $[0,1]$. The optimal eigenvalue remains a constant while b is changing. When $b > 1$, the optimal conductivities σ do not depend on x and are similar to the optimal solution on the interval $[0,b]$. The optimal eigenvalue is decreasing in b.

3.5. A circular domain. Consider the eigenvalue problem (2.1) on unit circle

$$\left\{(x,y) = x^2 + y^2 \leq 1\right\}.$$

We choose $\gamma = 0.1$, 0.4, and 0.9 to demonstrate how the optimal conductivities σ and their first nonzero eigenvalues λ vary with respect to γ. The results are shown in Figure 6. When $\gamma = 0.1$, the optimal conductivity has $D = \{x|\sigma(x) = \sigma_M\}$ consisting of two disjoint regions on two sides and $D^c = \{x|\sigma(x) = \sigma_m\}$ forms a nonconvex region in the middle. When $\gamma = 0.4$, the region with low conductivity

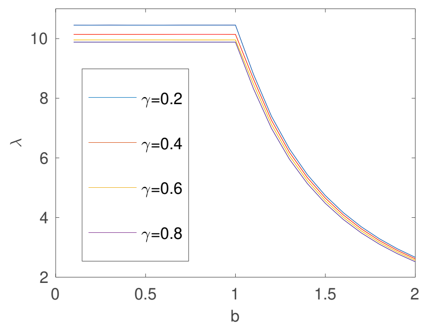

FIG. 5. *Dependence of optimal eigenvalue* λ *and length of shorter edges* b *on rectangular domains* $[0,1] \times [0,b]$ *with different* γ*.*

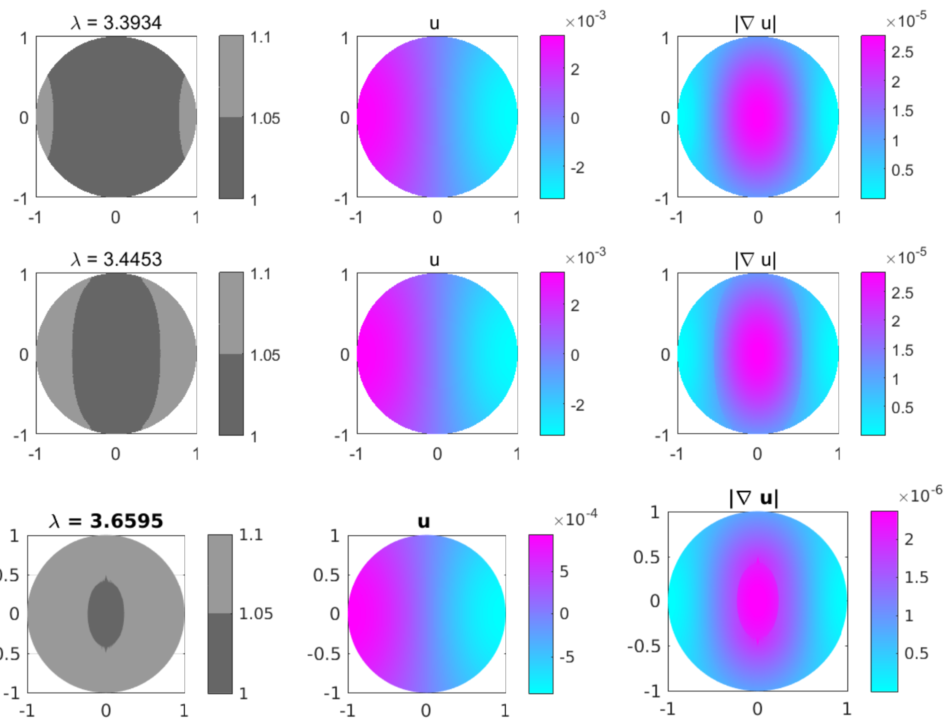

FIG. 6. *The optimal results on circular domains. From the left to right columns are shown the optimal conductivities* σ*, corresponding eigenfunctions, and absolute values of gradients of eigenfunctions with* $\gamma = 0.1, 0.4, 0.9$ *from the first row to the last row.*

$D^c = \{x|\sigma(x) = \sigma_m\}$ shrinks and becomes convex. When γ increases further, the region with low conductivity keeps shrinking and then no longer touches the boundary, and $D = \{x|\sigma(x) = \sigma_M\}$ becomes a connected domain. When $\gamma = 0.9$, the optimal conductivity distribution becomes a region made of σ_M material near the boundary and a region made of σ_m material in the middle of the disk.

3.6. An elliptical domain. Consider the eigenvalue problem (2.1) on an ellipse $\left\{(x,y) = \frac{x^2}{a} + \frac{y^2}{b} \leq 1\right\}$, where $a = 1$ and $b = 0.5$. We demonstrate how the optimal

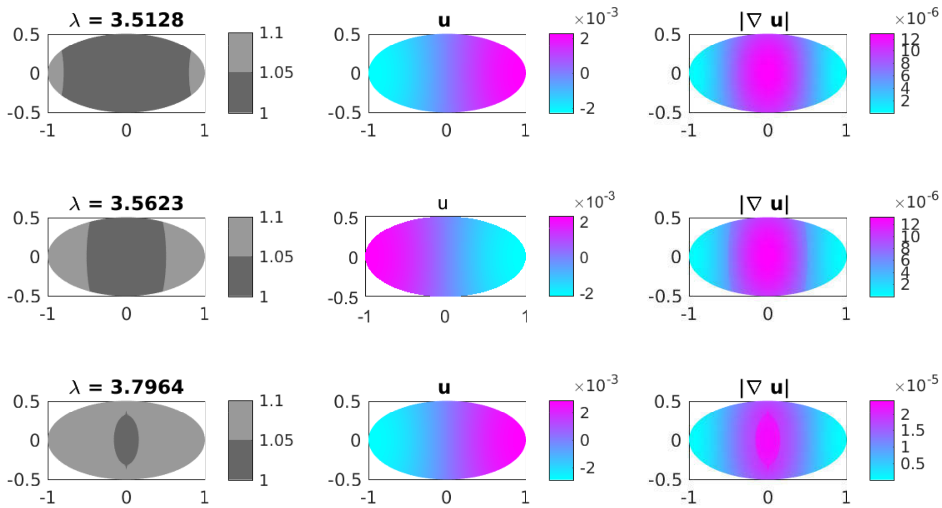

FIG. 7. *The optimal results on elliptical domains. From the left to right columns are shown the optimal conductivities σ, corresponding eigenfunctions, and absolute values of gradients of eigenfunctions. The ratio between two edges is 2 and $\gamma = 0.1, 0.4, 0.9$ from the first row to the last row.*

conductivities σ vary with respect to γ. Figure 7 shows results which are similar to those on a circular domain. When γ is small, the optimal σ is formed by two high conductivity regions near the end of longer edges and a low conductivity area in the middle. When γ is large, the low conductivity region will become small and disconnect with the boundary of the elliptical domain, and thus the optimal σ is formed by a high conductivity region near the boundary and low conductivity region in the middle.

3.7. Annular domains. Consider the eigenvalue problem (2.1) on annular domains $\{(x, y) : r^2 \leq x^2 + y^2 \leq 1\}$ with several different given r. We demonstrate how the optimal conductivities σ vary with respect to r and γ. The first four rows of Figure 8 present results for $r = 0.5$ with various choices of γ. When $\gamma = 0.05$, the high conductivity region of optimal σ is formed with four small parts, two of them adjacent to the outer boundary and two of them adjacent to the inner boundary. They are symmetrically distributed at two ends of a diameter. In this case, the low conductivity region is connected. When $\gamma = 0.1$, the high conductivity areas of σ are combined into two parts, and thus divide the low conductivity area into two parts as well. In the cases when $\gamma = 0.1$ and $\gamma = 0.4$, both high conductivity region and low conductivity region are disconnected. When $\gamma = 0.9$, the optimal σ is formed by two low conductivity regions adjacent to the inner boundary and one high conductivity region which is connected. The fifth row of Figure 8 shows the result when $r = 0.1$ and $\gamma = 0.6$. The optimal σ shows a different scenario when r is small.

3.8. L-shaped domains. Consider the eigenvalue problem (2.1) on L-shaped domains $([-1, 1] \times [-1, 1] \backslash ([k, 1] \times [k, 1])$. We examine the optimal conductivity distributions for different k and γ. We observe that the optimal conductivity configurations have the low conductivity region D^c always containing the corner point (k, k) even though it is hard to observe this in the first figure on the last row. The high conductivity region D always contains the corner point $(-1, -1)$. When $k = 0$, the low

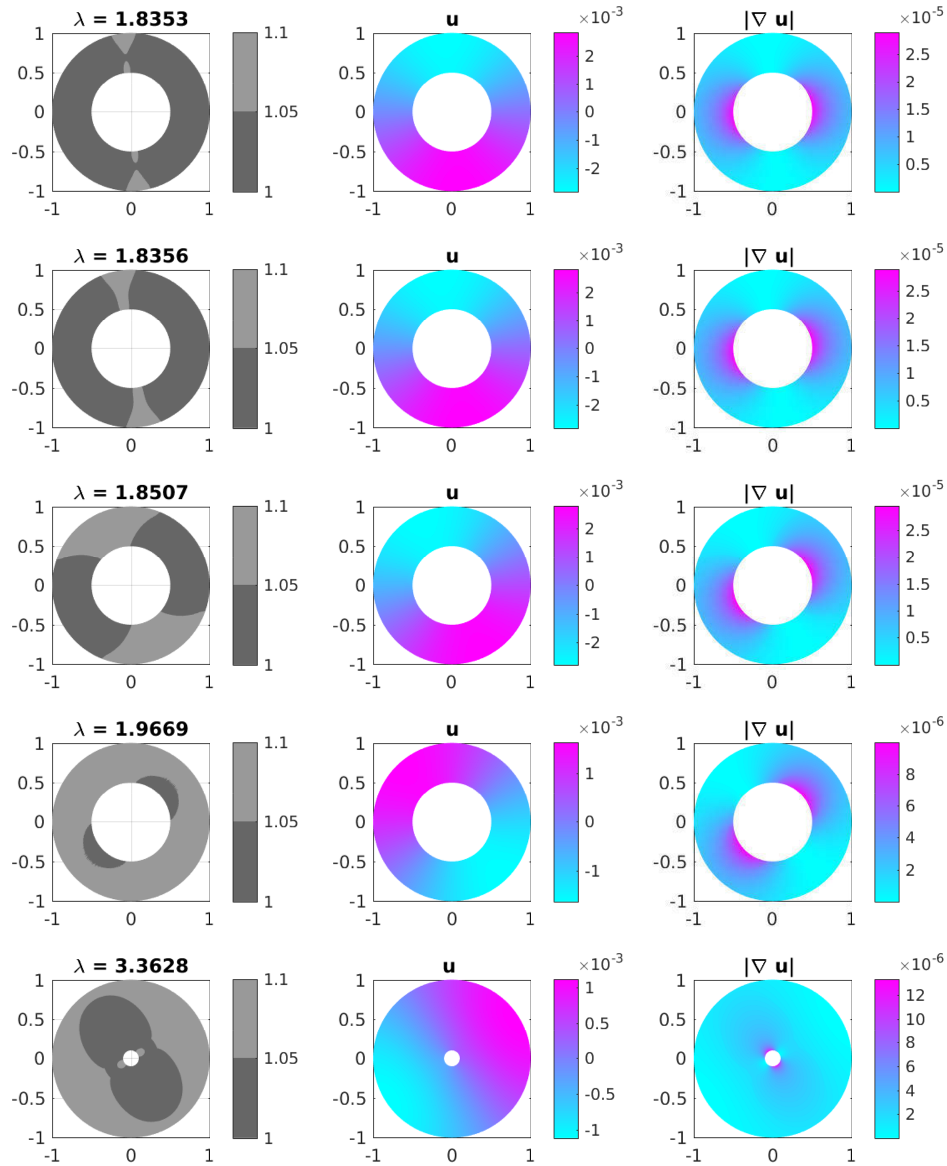

FIG. 8. *The optimal results on annular domains. From the left to right columns are shown the optimal conductivities σ, corresponding eigenfunctions, and absolute values of gradients of eigenfunctions. The first four rows are shown with the ratio between the outer radius and inner radius given by* 2 *and* $\gamma = 0.05, 0.1, 0.4, 0.9$. *In the fifth row,* $r = 0.1$ *and* $\gamma = 0.6$.

conductivity region is connected as shown in the first two rows in Figure 9. When $\gamma = 0.4$, the low conductivity region is connected with the bottom and left boundaries and thus divides the high conductivity region into three parts, as shown in the first row in Figure 9. When $\gamma = 0.8$, the low conductivity region is located in the middle and the high conductivity region is also connected. More scenarios and topological changes can be observed for wider L-shaped domain. In the case of $k = 0.8$, four different scenarios with respect to $\gamma = 0.2$, 0.3, 0.5, and 0.8 are shown in Figure 9

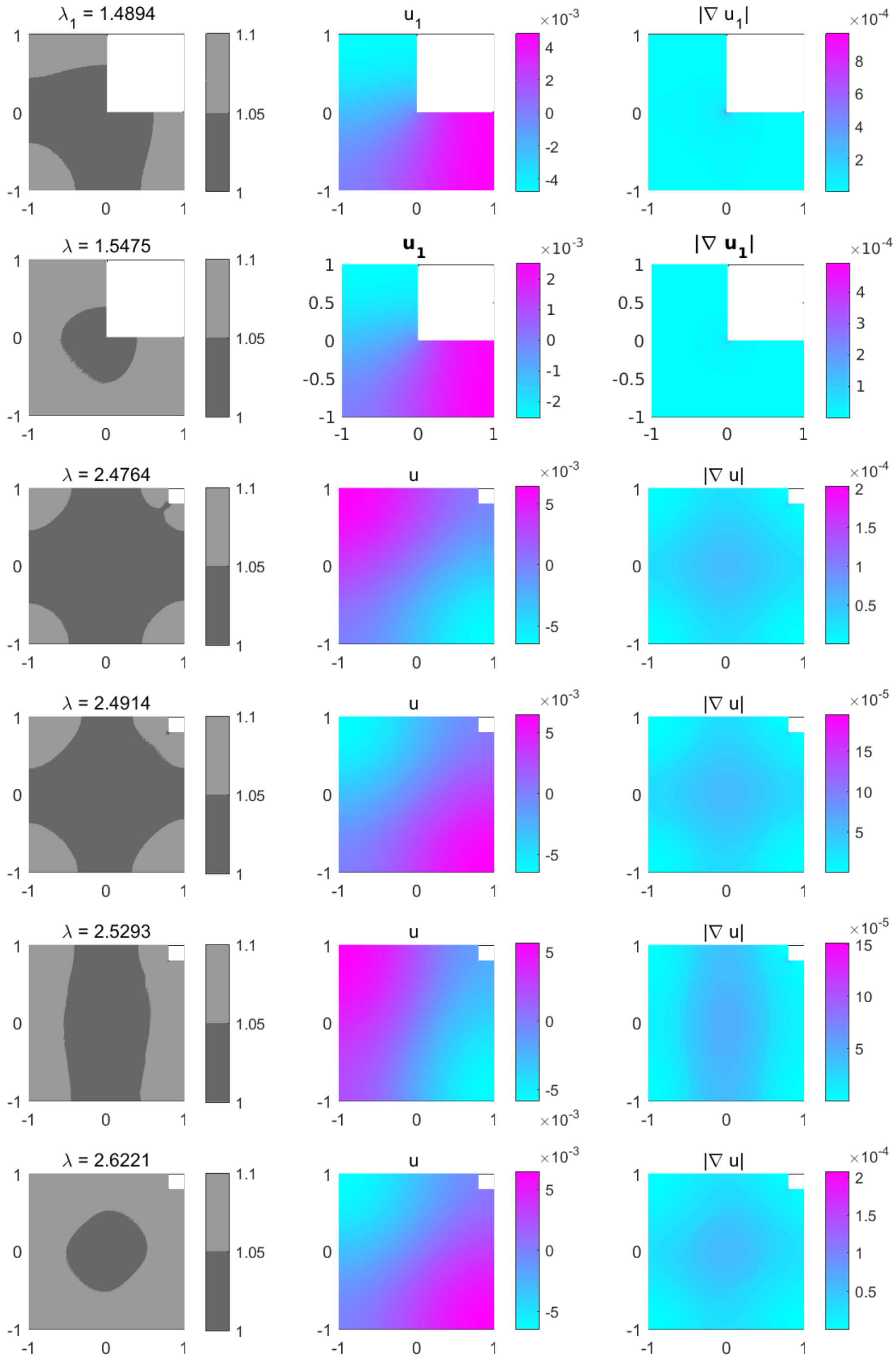

FIG. 9. *The optimal results on L-shaped domains. From the left to right columns are shown the optimal conductivities σ, the corresponding eigenfunctions, and absolute values of gradients of eigenfunctions. Results for $k = 0$ and $\gamma = 0.4$ and 0.8, respectively, are shown in the first and second rows; the results for $k = 0.8$ and $\gamma = 0.2$, 0.3, 0.5, and 0.8, respectively, are shown in the third row to the sixth row.*

from the third row to the sixth row. The high conductivity regions are divided into five, four, and two parts in the third, fourth, and fifth rows, respectively, and are connected in the sixth row. The low conductivity region is connected in the third row, while from the fourth to the sixth rows they are not connected due to the corner point $(0.8, 0.8)$. It is also worth noticing that the optimal σ for the third, fourth, and sixth rows have the same axis of symmetry as the L-shaped domain, i.e., the diagonal $y = x$, while in the fifth row there is no symmetric property for the optimal σ. In fact, in this case for the fifth row when $\gamma = 0.5$, a scenario similar to the fourth row provides another local minimizer, but the corresponding eigenvalue ($\lambda = 2.5336$) is higher than those shown in Figure 9 ($\lambda = 2.5293$).

4. Conclusion. In one dimension, we prove several monotone properties of eigenvalues. In addition, we have shown that the optimal conductivity distribution will have the high conductivity material placed evenly at two ends, and the low conductivity material placed in the middle of the interval, with the assumption that the low conductivity region is simply connected. This $\sigma_M - \sigma_m - \sigma_M$ spatial arrangement is not affected by varying σ_m or σ_M. The conductivity which achieves the minimal first nonzero eigenvalue of the Neumann problem is the same as the result which achieves the maximal first eigenvalue of the Dirichlet problem. It would be interesting to find out whether this particular optimal configuration is a global minimizer of (2.1) among materials which consist of two different conductivities with a prescribed area ratio.

In two-dimensional rectangular domains, we prove that the strip configuration can be a local minimizer by computing eigenvalues and eigenfunctions via method of separation of variables and studying their asymptotic behaviors. For general domains, the proposed rearrangement algorithm is able to obtain the minimizers σ on domains including squares, rectangular domains, circles, ellipses, annular domains, and L-shaped domains. On rectangular domains, the optimal material has the high conductivity material placed at two strips attached to the shorter edges and the low conductivity material placed in the middle of the domain. On a square, the optimizer is not unique due to its symmetry in both the x and y directions. We observe a similar phenomenon in other symmetrical shapes such as a circle and an annulus. On a circle or an ellipse, we observe that the low conductivity region could form a convex or nonconvex shape, and the high conductivity region may have different topologies depending on the area ratio. It would be interesting to find out when these kinds of shape and topology changes occur. On an annulus and L-shaped domain, we see the optimizers have many different configurations depending on the area ratio. Further analytical study is required to understand the properties of the optimizers and their relationship with their eigenfunctions. Last but not least, we observed numerically that the interface between the low conductivity and high conductivity regions may not be smooth. When do we expect the optimizer to have microstructural patterns? This challenging question has yet to be answered.

REFERENCES

[1] A. Alvino, G. Trombetti, and P. Lions, *On optimization problems with prescribed rearrangements*, Nonlinear Anal., 13 (1989), pp. 185–220.
[2] C. Anedda, F. Cuccu, and G. Porru, *Minimization of the first eigenvalue in problems involving the bi-Laplacian*, Rev. Mat. Teor. Apl., 16 (2009), pp. 127–136.
[3] D. O. Banks, *Bounds for the eigenvalues of nonhomogeneous hinged vibrating rods*, J. Math. Mech., 16 (1967), pp. 949–966.
[4] P. R. Beesack, *Isoperimetric inequalities for the nonhomogeneous clamped rod and plate*, J. Math. Mech, 8 (1959), pp. 471–482.

[5] L. Cadeddu, M. A. Farina, and G. Porru, *Optimization of the principal eigenvalue under mixed boundary conditions*, Electron. J. Differential Equations, 2014 (2014), pp. 1–17.

[6] J. Casado-Díaz, *A characterization result for the existence of a two-phase material minimizing the first eigenvalue*, Ann. Inst. H. Poincaré Anal. Non Linéaire, 34 (2017), pp. 1215–1226.

[7] S. Chanillo, D. Grieser, M. Imai, K. Kurata, and I. Ohnishi, *Symmetry breaking and other phenomena in the optimization of eigenvalues for composite membranes*, Comm. Math. Phys., 214 (2000), pp. 315–337, https://doi.org/10.1007/PL00005534.

[8] W. Chen, C.-S. Chou, and C.-Y. Kao, *Minimizing eigenvalues for inhomogeneous rods and plates*, J. Sci. Comput., 69 (2016), pp. 983–1013.

[9] W. Chen, K. Diest, C.-Y. Kao, D. E. Marthaler, L. A. Sweatlock, and S. Osher, *Gradient based optimization methods for metamaterial design*, in Numerical Methods for Metamaterial Design, Springer, 2013, pp. 175–204.

[10] M. Chugunova, B. Jadamba, C.-Y. Kao, C. Klymko, E. Thomas, and B. Zhao, *Study of a mixed dispersal population dynamics model*, in Topics in Numerical Partial Differential Equations and Scientific Computing, Springer, 2016, pp. 51–77.

[11] C. Conca, M. Dambrine, R. Mahadevan, and D. Quintero, *Minimization of the ground state of the mixture of two conducting materials in a small contrast regime*, Math. Methods Appl. Sci., 39 (2016), pp. 3549–3564.

[12] C. Conca, A. Laurain, and R. Mahadevan, *Minimization of the ground state for two phase conductors in low contrast regime*, SIAM J. Appl. Math., 72 (2012), pp. 1238–1259, https://doi.org/10.1137/110847822.

[13] C. Conca, R. Mahadevan, and L. Sanz, *An extremal eigenvalue problem for a two-phase conductor in a ball*, Appl. Math. Optim., 60 (2009), pp. 173–184.

[14] C. Conca, R. Mahadevan, and L. Sanz, *Shape derivative for a two-phase eigenvalue problem and optimal configurations in a ball*, ESAIM Proc., 27 (2009), pp. 311–321.

[15] S. Cox and R. Lipton, *Extremal eigenvalue problems for two-phase conductors*, Arch. Rational Mech. Anal., 136 (1996), pp. 101–117.

[16] S. J. Cox, *The two phase drum with the deepest bass note*, Japan J. Indust. Appl. Math., 8 (1991), pp. 345–355, https://doi.org/10.1007/BF03167141.

[17] S. J. Cox and D. C. Dobson, *Band structure optimization of two-dimensional photonic crystals in h-polarization*, Journal of Computational Physics, 158 (2000), pp. 214–224.

[18] S. J. Cox and D. C. Dobson, *Maximizing band gaps in two-dimensional photonic crystals*, SIAM J. Appl. Math., 59 (1999), pp. 2108–2120, https://doi.org/10.1137/S0036139998338455.

[19] F. Cuccu, B. Emamizadeh, and G. Porru, *Optimization of the first eigenvalue in problems involving the bi-Laplacian*, Proc. Amer. Math. Soc., 137 (2009), pp. 1677–1687.

[20] F. Cuccu and G. Porru, *Maximization of the first eigenvalue in problems involving the bi-Laplacian*, Nonlinear Anal., 71 (2009), pp. e800–e809.

[21] M. Dambrine and D. Kateb, *On the shape sensitivity of the first Dirichlet eigenvalue for two-phase problems*, Appl. Math. Optim., 63 (2011), pp. 45–74.

[22] L. He, C.-Y. Kao, and S. Osher, *Incorporating topological derivatives into shape derivatives based level set methods*, J. Comput. Phys., 225 (2007), pp. 891–909.

[23] A. Henrot, *Extremum Problems for Eigenvalues of Elliptic Operators*, Springer Science & Business Media, 2006.

[24] M. Hintermüller, C.-Y. Kao, and A. Laurain, *Principal eigenvalue minimization for an elliptic problem with indefinite weight and Robin boundary conditions*, Appl. Math. Optim., 65 (2012), pp. 111–146.

[25] D. Kang and C.-Y. Kao, *Minimization of inhomogeneous biharmonic eigenvalue problems*, Appl. Math. Model., 51 (2017), pp. 587–604.

[26] C.-Y. Kao, Y. Lou, and E. Yanagida, *Principal eigenvalue for an elliptic problem with indefinite weight on cylindrical domains*, Math. Biosci. Engrg., 5 (2008), pp. 315–335.

[27] C.-Y. Kao, S. Osher, and E. Yablonovitch, *Maximizing band gaps in two-dimensional photonic crystals by using level set methods*, Appl. Phys. B, 81 (2005), pp. 235–244.

[28] C.-Y. Kao and F. Santosa, *Maximization of the quality factor of an optical resonator*, Wave Motion, 45 (2008), pp. 412–427.

[29] C.-Y. Kao and S. Su, *Efficient rearrangement algorithms for shape optimization on elliptic eigenvalue problems*, J. Sci. Comput., 54 (2013), pp. 492–512.

[30] I. M. Karabash, *Nonlinear eigenvalue problem for optimal resonances in optical cavities*, Math. Model. Nat. Phenom., 8 (2013), pp. 143–155.

[31] M. G. Krein, *On certain problems on the maximum and minimum of characteristic values and on the Lyapunov zones of stability*, Amer. Math. Soc. Transl. (2), 1 (1955), pp. 163–187.

[32] J. Lamboley, A. Laurain, G. Nadin, and Y. Privat, *Properties of optimizers of the princi-*

pal eigenvalue with indefinite weight and Robin conditions, Calc. Var. Partial Differential Equations, 55 (2016), 144.

[33] A. Laurain, *Global minimizer of the ground state for two phase conductors in low contrast regime*, ESAIM Control Optim. Calc. Var., 20 (2014), pp. 362–388.

[34] J. Lin and F. Santosa, *Resonances of a finite one-dimensional photonic crystal with a defect*, SIAM J. Appl. Math., 73 (2013), pp. 1002–1019, https://doi.org/10.1137/120897304.

[35] Y. Lou and E. Yanagida, *Minimization of the principal eigenvalue for an elliptic boundary value problem with indefinite weight, and applications to population dynamics*, Japan J. Indust. Appl. Math., 23 (2006), pp. 275–292.

[36] M. Maksimović, M. Hammer, and E. B. van Groesen, *Coupled optical defect microcavities in one-dimensional photonic crystals and quasi-normal modes*, Opt. Engrg., 47 (2008), pp. 114601–114601.

[37] K. Matsue and H. Naito, *Numerical studies of the optimization of the first eigenvalue of the heat diffusion in inhomogeneous media*, Japan J. Indust. Appl. Math., 32 (2015), pp. 489–512.

[38] H. Men, K. Y. Lee, R. M. Freund, J. Peraire, and S. G. Johnson, *Robust topology optimization of three-dimensional photonic-crystal band-gap structures*, Opt. Express, 22 (2014), pp. 22632–22648.

[39] H. Men, N.-C. Nguyen, R. M. Freund, K.-M. Lim, P. A. Parrilo, and J. Peraire, *Design of photonic crystals with multiple and combined band gaps*, Phys. Rev. E, 83 (2011), 046703.

[40] F. Meng, B. Jia, and X. Huang, *Topology-optimized 3D photonic structures with maximal omnidirectional bandgaps*, Adv. Theory Simul., 1 (2018), 1800122.

[41] A. Mohammadi and M. Yousefnezhad, *Optimal ground state energy of two-phase conductors*, Electron. J. Differential Equations, 171 (2014), pp. 1–7.

[42] S. J. Osher and F. Santosa, *Level set methods for optimization problems involving geometry and constraints:* I. *Frequencies of a two-density inhomogeneous drum*, J. Comput. Phys., 171 (2001), pp. 272–288.

[43] B. Osting, *Bragg structure and the first spectral gap*, Appl. Math. Lett., 25 (2012), pp. 1926–1930.

[44] B. Schwarz, *Some results on the frequencies of nonhomogeneous rods*, J. Math. Anal. Appl., 5 (1962), pp. 169–175.

[45] O. Sigmund and K. Hougaard, *Geometric properties of optimal photonic crystals*, Phys. Rev. Lett., 100 (2008), 153904.